The Clay Minerals Society Workshop Lectures Series, Vol. 21 (2016), Chapter 12, 151–161

ON THE USE AND ABUSE OF N_2 PHYSISORPTION FOR THE CHARACTERIZATION OF THE PORE STRUCTURE OF SHALES

Pieter Bertier[1,*], Kevin Schweinar[1], Helge Stanjek[1], Amin Ghanizadeh[2], Christopher R. Clarkson[2], Andreas Busch[3], Niko Kampman[3], Dirk Prinz[4], Alexandra Amann-Hildenbrand[5], Bernhard M. Krooss[5], and Vitaliy Pipich[6]

[1]*Clay & Interface Mineralogy, RWTH-Aachen University, Bunsenstr. 8, D-52072 Aachen, Germany*
[2]*Department of Geoscience, University of Calgary, Calgary, Canada*
[3]*Shell Global Solutions International, Kessler Park 1, 2288 GS Rijswijk, The Netherlands*
[4]*Dynchem, Saarstrasse 98, D-52062 Aachen, Germany*
[5]*Institute for Petroleum & Coal, RWTH-Aachen University, Lochnerstr. 2, D-52062 Aachen, Germany*
[6]*Jülich Centre for Neutron Science JCNS, Forschungszentrum Jülich GmbH, Outstation at MLZ, Lichtenbergstrasse 1 85747 Garching, Germany*
[*]*e-mail: Pieter.Bertier@emr.rwth-aachen.de*

The use of N_2 physisorption for the characterization of the pore structure of shales is assessed by addressing some common pitfalls and misconceptions related to the interpretation of physisorption data. In addition, N_2 physisorption is compared to other methods used to characterize shales. For this purpose a set of pore-structure and total-porosity data from N_2 physisorption, He-pycnometry, Hg-intrusion porosimetry, fluid saturation (Archimedes) methods, and (ultra) small-angle neutron scattering was obtained from measurements on samples of Opalinus Clay.

1. Introduction

Porosity and pore structure are very important parameters in many geologic and engineering applications. With respect to shales and mudrocks, these properties are essential in the assessment of multiphase transport, geomechanical behavior, and storage/sealing capacity. Many methods are currently in use for the determination of porosity, each of which has advantages and disadvantages. Though porosity is theoretically an intrinsic property of a rock, different techniques often yield substantially different results. This is certainly the case for shales, in which substantial micro- (<2 nm), meso- (2–50 nm), as well as macro- (>50 nm) porosity is found. The lower range of pore sizes, in particular, makes it difficult to characterize porosity adequately by routine

DOI: 10.1346/CMS-WLS-21.12

methods such as those used for conventional reservoir rocks (*e.g.* petrography, X-ray micro-tomography, Hg-intrusion porosimetry).

The increase in commercial production of shale hydrocarbons over the past decade has resulted in a much-increased demand for porosity and pore-structure data for shales. To meet that demand, the geoscience research community has adopted methods from other disciplines which had proven useful in the characterization of micro- and mesoporous materials. One of those is N_2 physisorption analysis, a method which relies on physical adsorption of nitrogen gas at liquid nitrogen temperature (77 K). Adsorbed amounts of gas are measured (volumetrically or gravimetrically) as a function of relative pressure (absolute/saturation pressure). The resulting isotherms reflect mechanisms of pore filling, the physics of which can be used to infer pore volume and area distributions. N_2 physisorption analysis is an attractive method for characterizing shales because it is commercially available, inexpensive, and comes with commercial data-processing software which produces a myriad of information about the pore system of the samples being analyzed. The method was originally developed for applications in material sciences and physical chemistry (ceramics, catalysts, separation technology, pharmaceuticals, *etc.*). Substantial progress has been made recently in the interpretation of gas physisorption isotherms due to the development of novel engineered nanomaterials (reviewed by Thommes and Cychosz, 2014). These are ideal standards for characterizing physisorption mechanisms, because their pore structure is homogeneous and ordered, which allows for accurate quantitative assessment by diffraction methods.

CO_2 physisorption analysis is commonly used for characterization of micropores and is complementary to the N_2 method. Ar physisorption (at 87 K) has certain advantages over N_2 (Thommes and Cychosz, 2014), but to date it has not been applied much in shale characterization. These techniques will not be addressed further here.

2. Principles of N_2 physisorption

When nitrogen gas is in contact with a solid at 77 K, a specific number of gas molecules will be attracted to the surface of the solid by van der Waals forces (Thommes and Cychosz, 2014). This process is known as physical adsorption or physisorption. The interaction energy of physisorption is low, which distinguishes it from chemisorption (Rouquerol *et al.*, 2014). Physisorption is thermodynamically reversible at isothermal conditions, which is not the case for chemisorption. Chemisorption is insignificant in the case of N_2 on shales and so is not considered further here.

The number of physisorbed molecules depends on the relative pressure of the N_2 gas in equilibrium with it. Relative pressure (p/p_0) is the ratio of absolute gas pressure to saturation pressure, *i.e.* the pressure at which the unconfined gas condenses. The saturation pressure of N_2 at 77 K is 101.3 kPa because 77 K is the boiling point of N_2. At a given relative pressure, the amount of gas at a specific part of the surface of a solid depends on local surface-energetic properties and on the geometry of the surface. To interpret physisorption measurements of porous systems, surfaces are classically

assumed to be homogeneous, so the amount adsorbed at a specific relative pressure is determined by pore size/geometry. These two aspects are clearly intimately related, so assumptions have to be made about geometry to obtain pore size. The most common assumption is that of a cylindrical pore system. At low pressures ($p/p_0 < 0.2$), micropores are filled with N_2; as pressure increases mesopores fill; and from $\sim p/p_0 = 0.96$, macropores are filled. Theoretically, at $p/p_0 = 1$ all pores are filled, but in practice this implies that the free space in the measurement cell is filled with N_2, so high relative pressures yield no relevant information (Rouquerol *et al.*, 2014). Specific relative pressure ranges are associated with specific adsorption mechanisms. Desorption of N_2 occurs partly by different mechanisms. Physical models of these adsorption and desorption mechanisms constitute the basis for the interpretation of isotherms in terms of porosity and pore structure.

3. Data-processing methods and their applicability to shale samples

N_2 physisorption isotherms hold a wealth of information about surface area and energy; only the theories used for the extraction of porosity and pore structure of shales will be addressed here.

The simplest way to extract porosity information from N_2 isotherms is by use of Gurvich's rule (Rouquerol *et al.*, 2014) which states that the amount adsorbed at the limiting plateau of an isotherm is a measure of the total adsorption capacity, and to obtain the corresponding total pore volume, the adsorbate can be assumed to have the molar volume of the liquid at the operational temperature. Gurvich's rule was developed for mesoporous materials (Gurvich, 1915), restricting its applicability for micro- and macroporous materials such as shales. The presence of micropores results in inaccurate total pore volumes because of molecular sieving by smaller micropores and deviations from the liquid density in micropores (positive or negative, depending on the material) (Thommes, 2010). Isotherms of macroporous materials do not have limiting plateaus corresponding to the maximum adsorption capacity. The isotherms increase asymptotically toward $p/p_0 = 1$, which makes the Gurvich total pore volume very sensitive to the choice of the relative pressure point. This can be overcome pragmatically by assigning a pore diameter to the selected relative pressure (*e.g.* by use of the Kelvin equation), and reporting it together with the 'total' pore volume. Several papers on shales report Gurvich pore volumes for pore diameters below $\sim$0.35 μm, corresponding to a relative pressure of $\sim$0.995 (*e.g.* Rexer *et al.*, 2013; Mastalerz *et al.*, 2013; Chen *et al.*, 2014; Liu *et al.*, 2015; Cao *et al.*, 2015). The reported pore volumes are specific, *i.e.* in cm^3/g, while porosity is generally desired as a volume fraction. This implies that an extra measurement of grain density is required for which He-pycnometry data can be used, or a value calculated from the mineral composition of the sample, if available.

The Barrett-Joyner-Halenda (BJH, Barrett *et al.*, 1951) method is used widely to calculate the pore-volume (and area) size distribution (PSD, *i.e.* the pore volume or surface

area associated with each pore size range) of shales. This method relies on the Kelvin equation which describes the effect of surface curvature of a liquid–vapor meniscus on the vapor pressure and thus relates pore diameter to relative pressure. For practical use in N_2 physisorption, unconnected cylindrical pore geometry is assumed, so the resulting PSD represents an equivalent capillary bundle, analogous to mercury intrusion porosimetry. Because the Kelvin equation describes capillary condensation phenomena, its relevance is restricted to the relative pressure range where those occur, *i.e.* to meso- and smaller macropores. The Kelvin radius is the radius of a meniscus, not the pore radius, because pore walls are lined with layer(s) of adsorbate before capillary condensation occurs. The BJH radius is, therefore, the sum of the Kelvin radius and the statistical thickness of the adsorbate layer. For smaller mesopores during adsorption, in particular, this statistical thickness (t) contributes substantially to the BJH radius. Several models are used to calculate t and these are based on measurements of non-porous reference materials and theoretical considerations. The Harkins-Jura equation, based on Al_2O_3 (Harkins and Jura, 1944), has been suggested to be appropriate for analysis of shales (Kuila and Prasad, 2013). Comparison based on an extensive shale data set showed that the choice of the t model does not make a significant difference if the BJH theory is applied within the p/p_0 where it is valid.

The range of validity of the BJH theory is a crucial issue, which, all too often, is ignored or misconceived by researchers working with shales. Firstly, adsorption and desorption in mesoporous materials such as shales, happen by different mechanisms. This is shown by pronounced hysteresis of the N_2 isotherms at $p/p_0 > 0.42$. During adsorption, pores fill gradually by molecules adsorbing in layers of increasing thickness on pore walls. In the course of desorption, the same pores empty by withdrawing menisci at the gas–liquid interface. This is an oversimplification, but it illustrates the concepts. Both isotherm branches can be used to obtain BJH PSD, but they yield different information. Research on engineered materials containing spherical pores with cylindrical throats, for example, showed that desorption is determined by throats, while adsorption holds information on the pore bodies (Thommes, 2010). For complex systems of pores, covering broad ranges of diameters and shapes, randomly organized in networks as in shales, the explanation of the difference between adsorption and desorption data is less trivial but must be considered in the interpretation of the PSD.

The menisci controlling desorption become unstable at $p/p_0 = 0.42$ for N_2 at 77 K. This is classically considered as an inherent property of the fluid (and T, the 'tensile strength effect,' Groen *et al.*, 2003) but was recently shown to depend to some extent on pore size (Thommes *et al.*, 2006; Rasmussen *et al.*, 2010). The forced closure of the hysteresis loop at $p/p_0 = 0.42$ produces an artefact in BJH PSD, *i.e.* a spike or steep slope at $\sim$3.8 nm in differential and cumulative distributions, respectively. This artefact makes up a substantial part of the pore volume of shales. Though this is well established, recent papers on shales often interpret it as a rock property (*e.g.* Olabode and Radonjic, 2014; Cao *et al.*, 2015; Tang *et al.*, 2015). Adsorption data are not affected by this artefact, but are subject to other issues. Studies on engineered materials showed that BJH underestimates the pore size by up to 20–30% for mesopores which are $<$10 nm in size (Thommes, 2004).

The most advanced and accurate methods to analyze pore structures from physisorption data are based on density functional theory (DFT) or Monte Carlo simulations of molecular dynamics (MC) (for reviews, see Thommes, 2010 or Rouquerol *et al.,* 2014). The DFT or MC is used to calculate the pressure dependency of density profiles for N_2 confined in pores with specific geometries in specific solids. This enables calculation of reference isotherms for specific pore systems. By varying pore-size parameters, these calculated isotherms are fitted iteratively to measured data. This procedure was shown to produce excellent results for engineered materials. For those, pore-size and geometry parameters can be constrained sufficiently to obtain unique fits. For compositionally heterogeneous materials with complex pore systems, such as shales, this is not the case. Experimental data can be fitted perfectly, but the results are unreliable. At present, none of the available kernels (gas-solid-geometry models) is suitable for (organic-rich) shales. Despite warnings from developers against application of their kernels for systems other than those for which they were designed, many geoscientists seem to interpret the numbers produced without much consideration. Fortunately, new and more complex kernels are being released at an increasing pace, and it is likely that in the near future DFT-MC models suitable for shale analysis will be developed.

4. The conundrum of low-pressure hysteresis

Several recent physisorption studies on shales report N_2 isotherms displaying a hysteresis at $p/p_0 < 0.42$, but none has addressed it specifically in adequate detail (*e.g.* Kuila and Prasad, 2013; Mastalerz *et al.*, 2013; Chen and Xiao, 2014; Cao *et al.*, 2015). Handbooks are quite clear about low-pressure hysteresis (LPH): any hysteresis below this pressure violates the thermodynamics of equilibrium physisorption, and should, therefore, be related to chemisorption, structural deformation of the sample, or lack of thermodynamic equilibrium (Rouquerol *et al.*, 2014). In all of those cases, physisorption-based theories are invalid. Systematic analyses of the present shale sample set showed that this LPH is most common for mature black shales, and is perfectly reproducible. The latter implies that chemisorption and deformation can be excluded.

The lack of an equilibrium hypothesis was tested and confirmed by systematic physisorption measurements with different equilibration times, on a shale sample (200–400 μm particle-size fraction) showing substantial LPH (Figure 1a). N_2 physisorption isotherms were measured with different equilibration criteria. Equilibrium was assumed when the pressure change per equilibration time interval was $<0.01\%$ of the average pressure during this interval. Equilibration time intervals were between 10 and 60 s (total isotherm measurement times = 8–40 h). These results show that even at very long equilibration times the hysteresis loop does not close at low pressures. Longer equilibration times resulted in larger amounts adsorbed for both the adsorption and desorption branches over the entire relative pressure range. For one isotherm (Figure 1a: orange, 20 s equilibration time) 50 closely spaced data points between 0.30 and 0.31 were recorded during adsorption and desorption, which implies that the sample was kept at relatively constant pressure for 7 h during adsorption and 4 h

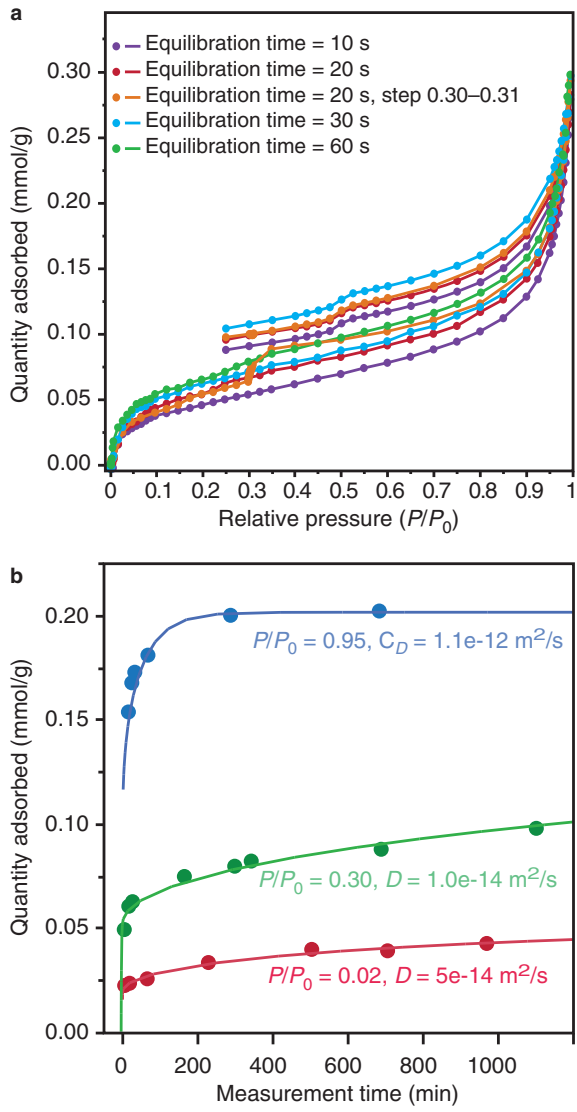

Figure 1. (a) N_2 physisorption isotherms of a shale sample (200–400 μm fraction), displaying substantial low-pressure hysteresis, measured with different equilibration criteria. Equilibration time intervals were between 10 and 60 s (total isotherm measurement times: 8–40 h). These results show that even at very long equilibration times the hysteresis loop does not close at low pressures which confirms that shale samples displaying low-pressure hysteresis do not attain sorption equilibrium during measurement. (b) Amount adsorbed as a function of time, measured (circles) at constant relative pressure, on the aliquot of shale from Figure 1a. The lines are fits to the data points, of the analytical solution of Fick's Law (100 summation terms), for diffusion into a sphere ($r = 150$ μm), for which the effective diffusion coefficients (D) obtained are displayed. The low values for D over the entire relative pressure ranges suggest strong diffusion control on the adsorption process.

during desorption. The adsorption branch shows a pronounced step in this p/p_0 range, while desorption is unaffected. These findings confirm that shale samples displaying LPH do not attain sorption equilibrium within reasonable measurement times.

The amount of N_2 adsorbed is very time dependent for samples displaying LPH. The relation between amount adsorbed at constant relative pressure and time was fitted by Fick's second law for diffusion into a sphere (Crank, 1975), yielding low, but reasonable, effective diffusion coefficients (10^{-14}–10^{-12} m^2/s) for N_2 in shales at 77 K (Figure 1b).

These results imply that either a substantial amount of pore volume is present in ultramicropores in which N_2 diffusion is very slow, or that part of the pore volume is only accessible through very small such pores. In practice this implies that the pore volume of shales displaying LPH could be substantially underestimated.

5. Comparison of results from N_2 physisorption with those from other methods

5.1. Materials and methods

Porosity and PSD results from N_2 physisorption were compared with results from He-pycnometry, Hg-intrusion porosimetry, water saturation, and small-angle neutron scattering for a set of nine samples of Opalinus Clay (Figure 2). These were taken from a 2 m section of homogeneous core from the Mont Terri laboratory (Switzerland). Mineral quantification was performed by Rietveld refinement, using the *Profex-BGMN* software (Doebelin and Kleeberg, 2015), of X-ray diffraction (Huber MC9300, HUBER Diffraktionstechnik GmbH & Co. KG, Rimsting, Germany) patterns recorded on randomly oriented bulk samples. X-ray fluorescence spectrometry (Spectro XLab2000, SPECTRO Analytical Instruments GmbH, Kleve, Germany) was used for bulk chemical analysis of the major and minor elemental compositions. In addition, the cation-exchange capacities of the samples were measured by photospectrometric determination of the CuTrien uptake of crushed samples in suspension. Details of these characterization methods and data were given by Amann-Hildenbrand *et al.* (2015). Mineralogical and chemical analysis confirmed the low heterogeneity of the sample set.

He-pycnometry, Hg-intrusion, and water-saturation methodologies were listed by Amann-Hildenbrand *et al.* (2015); small angle neutron scattering (SANS) measurement conditions were identical to those of Kampman *et al.* (2016). The pore-size ranges of the applied methods accessed are summarized in Figure 2.

N_2 physisorption analysis was performed using a Micromeritics Gemini VII 2390t device (Micromeritics Instrument Corporation, Norcross, Georgia, USA), by means of the static volumetric method, in a liquid N_2 bath. A crushed fraction of 63–400 μm, prepared manually in a mortar with minimal use of energy to avoid strain, was measured. The samples were outgassed at 130°C below 3 Pa for >24 h. Adsorption was measured at 42 relative pressure steps between 0.001 and 0.995 and desorption at 29 relative pressure points between 0.995 and 0.1. The nitrogen saturation pressure (p_0)

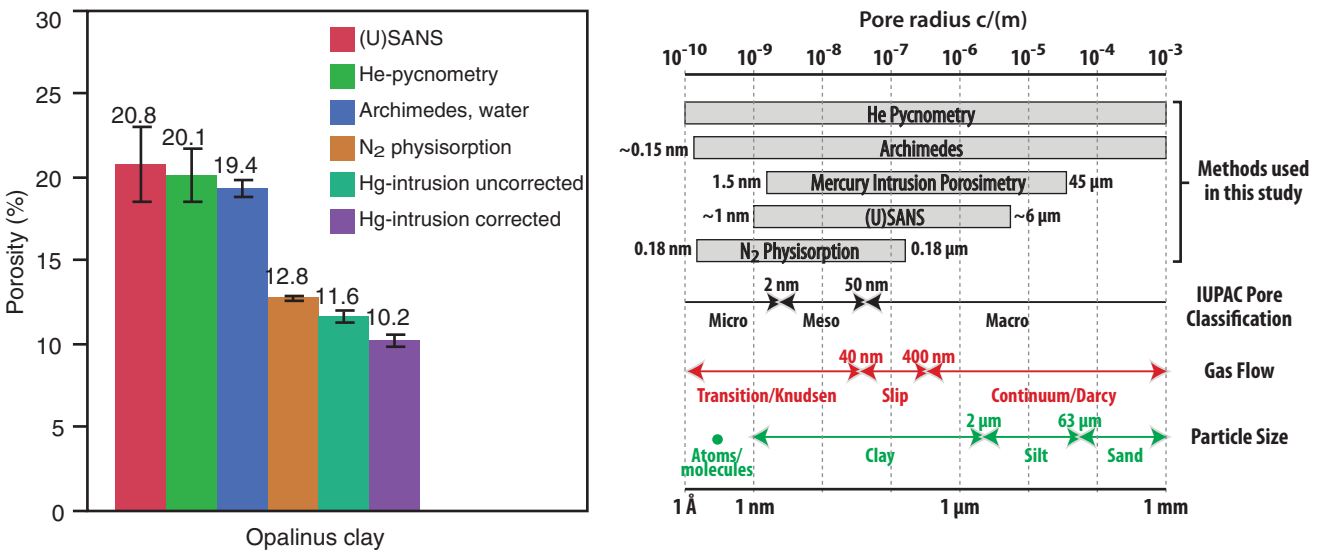

Figure 2. Comparison of the average porosities (vol.%, ± 2 standard deviations) of nine Opalinus Clay samples (Mont Terri, Switzerland) measured by combined Small-angle neutron scattering–ultra-small-angle neutron scattering (SANS-USANS), He-pycnometry, Archimedes' method (water saturation), N_2 physisorption (Gurvich pore volume, max. pore diameter = 0.35 µm), and Hg-intrusion porosimetry (with or without correction for surface roughness, see Amann-Hildenbrand *et al.*, 2015). These samples were taken from a 2 m long, homogeneous section of core. The mineralogy and chemical composition were presented by Amann-Hildenbrand *et al.* (2015).

was determined separately for each relative pressure point. Sorbate-sorbent equilibrium was assumed when the pressure change over a 10 s interval was $<0.01\%$ of the average pressure during the latter interval. Gurvich pore volumes were calculated from the p/p_0 point at 0.995 (BJH diameter of ~ 0.35 μm) assuming liquid nitrogen density (28.8 mol/L). Porosities were calculated from specific pore volumes using the grain density from He-pycnometry.

6. Results

The average porosity of the nine samples studied, and its variability over the sample set, are summarized in Figure 2, for each of the porosimetric techniques applied. The results of N_2 porosity data are between 40 and 60% of the He-pycnometry values. Helium, as a very small molecule with low affinity for solids, is likely to access all pores during pycnometry, which is not the case for N_2. Water saturation yielded porosities similar to He-pycnometry for samples saturated under confinement in a triaxial cell. The samples studied contain swelling clays (illite-smectite mixed-layer clays) but have small cation exchange capacities (150 μmol/g). No substantial swelling due to water saturation was observed. Total porosity values from Hg-porosimetry are smaller than the N_2 data for all samples, though the method accesses a broader range of pore sizes (1.5 nm–45 μm). This might be due to compression of the samples at the high isotropic pressure applied during measurement (Clarkson *et al.*, 2013). (U)SANS data, covering a pore-size range of 2 nm to 10 μm, correspond well to He-pycnometry. Pore-size distribution data from neutron scattering are in fair agreement with those from N_2, while Hg-intrusion gave very different PSD values, in the pore-size range of overlap.

This unique data set of shale porosities from different measurement techniques shows clearly that although the individual techniques are reasonably precise, the accuracy of porosity measurements is problematic. The inaccuracy is related partly to the different pore-size ranges assessed by the specific methods, yet this does not explain all of the differences quantitatively.

7. Summary and conclusions

N_2 physisorption is a useful technique in the analysis of the pore structure of shales and mudrocks, but the results should be interpreted with caution:

(1) Gurvich total pore volumes do not represent the total porosity of shales because N_2 physisorption does not yield information about pores larger than ~ 0.35 μm and the density of N_2 in micropores differs from that of liquid N_2 at 77 K.

(2) Barrett-Joyner-Halenda (BJH) pore-size distributions from desorption isotherms represent pore-throat sizes and should not be used for pores smaller than 4 nm, due to artefacts related to the forced closure of capillary hysteresis loops. Pore-size distributions from adsorption isotherms give information about pore bodies. BJH data underestimate substantially the volumes of pores of <10 nm in size.

(3) Low-pressure hysteresis observed mainly for organic-rich shales is related to incomplete equilibration during measurements, due to slow diffusion in small micropores and restricted access to significant fractions of pore volume through micropores. Inversion of isotherms displaying low-pressure hysteresis gives inaccurate information on pore structures.

(4) Gurvich pore volumes for pores smaller than 0.35 μm, calculated from N_2 physisorption on a set of Opalinus Clay samples, correspond to 40–60% of the values of porosity from He-pycnometry, neutron scattering, and water saturation. Hg-intrusion total porosities are lower than N_2 physisorption values. Pore-size distributions using BJH correspond fairly well to those from neutron scattering, but differ substantially from Hg-intrusion.

Acknowledgments

Guest editor: Reiner Dohrmann

The authors and editors are grateful to anonymous reviewers who offered very helpful input and suggestions. A list of all reviewers is given at the end of the Preface for this volume.

References

Amann-Hildenbrand, A., Krooss, B.M., Busch, A., and Bertier, P. (2015) Laboratory testing procedure for CO_2 capillary entry. Pp. 355–384 in: *Carbon Dioxide Capture for Storage in Deep Geological Formations*, Vol. **4** (K.F. Gerdes, editor). CPL Press and BPCNAI.

Barrett, E.P., Joyner, L.G., and Halenda, P.P. (1951) The determination of pore volume and area distributions in porous substances. I. Computations from nitrogen isotherms. *Journal of the American Chemical Society*, **73**, 373–380.

Cao, T., Song, Z., Wang, S., and Xia, J. (2015) A comparative study of the specific surface area and pore structure of different shales and their kerogens. *Science China Earth Sciences*, **58**, 510–522.

Chen, J. and Xiao, X. (2014) Evolution of nanoporosity in organic-rich shales during thermal maturation. *Fuel*, **129**, 173–181.

Chen, Y., Wei, L., Mastalerz, M., and Schimmelmann, A. (2014) The effect of analytical particle size on gas adsorption porosimetry of shale. *International Journal of Coal Geology,* **138**, 103–112.

Clarkson, C.R., Solano, N., Bustin, R.M., Bustin, A.M.M., Chalmers, G.R.L., He, L., Melnichenko, Y.B., Radliński, A.P., and Blach, T.P. (2013) Pore structure characterization of North American shale gas reservoirs using USANS/SANS, gas adsorption, and mercury intrusion. *Fuel*, **103**, 606–616.

Crank, J. (1975) *The Mathematics of Diffusion*, 2nd edition. Clarendon Press, Oxford, UK, 414 pp.

Doebelin, N. and Kleeberg, R. (2015) Profex: a graphical user interface for the Rietveld refinement program BGMN. *Journal of Applied Crystallography*, **48**, 1573–1580.

Groen, J.C., Peffer, L.A., and Pérez-Ramírez, J. (2003) Pore size determination in modified micro- and mesoporous materials: Pitfalls and limitations in gas adsorption data analysis. *Microporous and Mesoporous Materials*, **60**, 1–17.

Gurvich, L.G. (1915) On the physico-chemical force of attraction. *Journal of the Physical and Chemical Society of Russia*, **47**, 805–827 (in Russian).

Harkins, W.D. and Jura, G. (1944) Surfaces of solids. XIII. A vapor adsorption method for the determination of the area of a solid without the assumption of a molecular area, and the areas occupied by nitrogen and other molecules on the surface of a solid. *Journal of the American Chemical Society*, **66**, 1366–1373.

Kampman, N., Busch, A., Bertier, P., Snippe, J., Hangx, S., Pipich, V., Di, Z., Rother, G., Harrington, J., Evans, J.P., Maskell, A., Chapman, H.J., and Bickle, M.J. (2016) Observational evidence for the long-term integrity of CO_2-reservoir caprocks. *Nature Communication,* in press.

Kuila, U. and Prasad, M. (2013) Application of nitrogen gas-adsorption technique for characterization of pore structure of mudrocks. *The Leading Edge*, **32**, 1478–1485.

Liu, X., Xiong, J., and Liang, L. (2015) Investigation of pore structure and fractal characteristics of organic-rich Yanchang formation shale in central China by nitrogen adsorption/desorption analysis. *Journal of Natural Gas Science and Engineering*, **22**, 62–72.

Mastalerz, M., Schimmelmann, A., Drobniak, A., and Chen, Y. (2013) Porosity of Devonian and Mississippian New Albany Shale across a maturation gradient: Insights from organic petrology, gas adsorption, and mercury intrusion. *AAPG Bulletin*, **97**, 1621–1643.

Olabode, A., and Radonjic, M. (2014) Characterization of shale cap-rock nano-pores in geologic CO_2 containment. *Environmental & Engineering Geoscience*, **20**, 361–370.

Rasmussen, C.J., Vishnyakov, A., Thommes, M., Smarsly, B.M., Kleitz, F., and Neimark, A.V. (2010) Cavitation in metastable liquid nitrogen confined to nanoscale pores. *Langmuir*, **26**, 10147–10157.

Rexer, T.F., Benham, M.J., Aplin, A.C., and Thomas, K.M. (2013) Methane adsorption on shale under simulated geological temperature and pressure conditions. *Energy & Fuels*, **27**, 3099–3109.

Rouquerol, F., Rouquerol, J., Sing, K.S.W., Llewellyn, P., and Maurin, G. (2014) *Adsorption by Powders and Porous Solids: Principles, Methodology and Applications*, 2nd edition. Academic Press, Oxford, UK, 630 pp.

Tang, X., Zhang, J., Jin, Z., Xiong, J., Lin, L., Yu, Y., and Han, S. (2015) Experimental investigation of thermal maturation on shale reservoir properties from hydrous pyrolysis of Chang 7 shale, Ordos Basin. *Marine and Petroleum Geology*, **64**, 165–172.

Thommes, M. (2004) Physical adsorption characterization of ordered and amorphous mesoporous materials. Pp. 317–364 in: *Nanoporous Materials: Science and Engineering* (G.Q. Lu and X.S. Zhao, editors). Imperial College Press, London, UK.

Thommes, M. (2010) Physical adsorption characterization of nanoporous materials. *Chemie Ingenieur Technik*, **82**, 1059–1073.

Thommes, M. and Cychosz, K. (2014) Physical adsorption characterization of nanoporous materials: Progress and challenges. *Adsorption*, **20**, 233–250.

Thommes, M., Smarsly, B., Groenewolt, M., Ravikovitch, P.I., and Neimark, A.V. (2006) Adsorption hysteresis of nitrogen and argon in pore networks and characterization of novel micro- and mesoporous silicas. *Langmuir*, **22**, 756–764.